An optofluidic device for surface enhanced Raman spectroscopy†

Miao Wang,[a] Nan Jing,[a] I-Hsien Chou,[b] Gerard L. Cote[b] and Jun Kameoka*[a]

Received 12th December 2006, Accepted 5th February 2007
First published as an Advance Article on the web 28th February 2007
DOI: 10.1039/b618105h

We have developed an optofluidic device that improves the sensitivity of surface enhanced Raman spectroscopy (SERS) when compared to other SERS approaches. This device has a pinched and step microchannel–nanochannel junction that can trap and assemble nanoparticles/target molecules into optically enhanced SERS active clusters by using capillary force. These SERS active clusters provide an electromagnetic enhancement factor of $\sim 10^8$. In addition, due to the continuous capillary flow that can transport nanoparticles/target molecules into the junction sites, the numbers of nanoparticles/target molecules and SERS active sites are increased. As a result, the detection limit of SERS for adenine molecules was better than 10 pM.

Introduction

SERS has been studied for decades as a means to enhance the Raman cross section of a molecule, and thus has the potential to provide a label-free analytical technique for characterizing molecular structure information.[1–9] Target molecules are adsorbed onto ''SERS-active structures'', such as roughened electrodes[10,11] or silver or gold nanoparticles,[2–7,9] which can provide a great deal of electromagnetic and chemical enhancement[2,12–14] at SERS-active sites[2,4,8,15] when they are exposed to the excitation laser source. However, because of the non-uniform distribution of these SERS-active sties, it is especially challenging to get controllable and consistent enhancement. This inconsistent enhancement is one of the reasons that SERS has not provided reliable and reproducible results in the past. In addition, target molecules are randomly adsorbed on the nanoparticle clusters. This means that the probability that target molecules are confined in a SERS-active site is low. These problems have limited the expansion of SERS applications. To improve the SERS technique, there are some new investigations underway. For instance, metal nanoparticle-array plates that have periodically aligned nanoparticles on the detection site were investigated as SERS-active substrates in an effort to provide reliable results.[16–19] Also, a nanoparticle-film with temperature-controllable inter-particle spacing was designed as a tunable SERS substrate to generate optimal SERS signal intensity.[20] Other substrates, such as metal-film-over-nanospheres (MFON)[21] and nanowell surfaces in microfluidic biochips,[22] have been reported. Metal nanoshells[23] and nanorods[24] have also been investigated as SERS-active substrates. However, all of these approaches take a long time for the molecules to adsorb on the SERS active site. In addition, the distribution of molecular adsorption on the SERS active site at low sample concentration is not uniform.

To overcome these limitations, a novel optofluidic molecule/particle trapping device that can improve the SERS signal is developed and described in this paper. This device has a pinched and step microfluidic–nanochannel junction where metallic nanoparticles and target molecules in aqueous solution can be reproducibly trapped to form nanoparticle–molecule SERS clusters using capillary force in the channel. This optofluidic device has three advantages. It has higher sensitivity because of an increased local density of nanoparticle/target molecules. Secondly, the device does not require chemical agents or salts to initiate the aggregation of nanoparticles. Thirdly, the device has higher reproducibility because SERS active clusters are consistently formed at a specific location namely, the entrance of the nanochannel.

Experimental

The optofluidic device was fabricated on a 500 μm-thick double-side-polished borosilicate wafer using photolithographic and etching processes. The device has a step structure consisting of a deep microchannel and a shallow nanochannel. The shallow channel has a 40 nm depth, 5 μm width, and 40 μm length, which is used for trapping nanoparticles with a diameter of 60 nm at the microchannel–nanochannel junction. The device was defined by photolithography and patterned by a reactive ion etching process. The deep channel had a 6 μm depth, 150 μm width, and was defined by photolithography and patterned by a wet HF etching process. After the wet etching process, inlet holes were made by a sand-blaster through the substrate wafer, which was bonded to another flat borosilicate wafer to seal the trenches and create the fluidic channels. Two plastic reservoirs were attached on both inlet holes. The schematic diagrams of this device are shown in Fig. 1(a) and (b). Immediately after a sample solution was dispensed in the channel, the gold nanoparticles with target molecules were transported and trapped at the nanochannel entrance due to the capillary force. The schematic diagram of this phenomenon is shown in Fig. 1(c). To confirm the trapping capability of this device, fluorescent polystyrene (PS)

[a]*Department of Electrical and Computer Engineering, Texas A&M University, College Station, TX, 77843-3128, USA. E-mail: kameoka@ece.tamu.edu; Fax: +1 979-845-6259; Tel: +1 979-845-7564*
[b]*Department of Biomedical Engineering, Texas A&M University, College Station, TX, 77843-3120, USA*

† Electronic supplementary information (ESI) available: Investigations of the formation of gold nanoparticle clusters at the entrance of the nanochannel. See DOI: 10.1039/b618105h

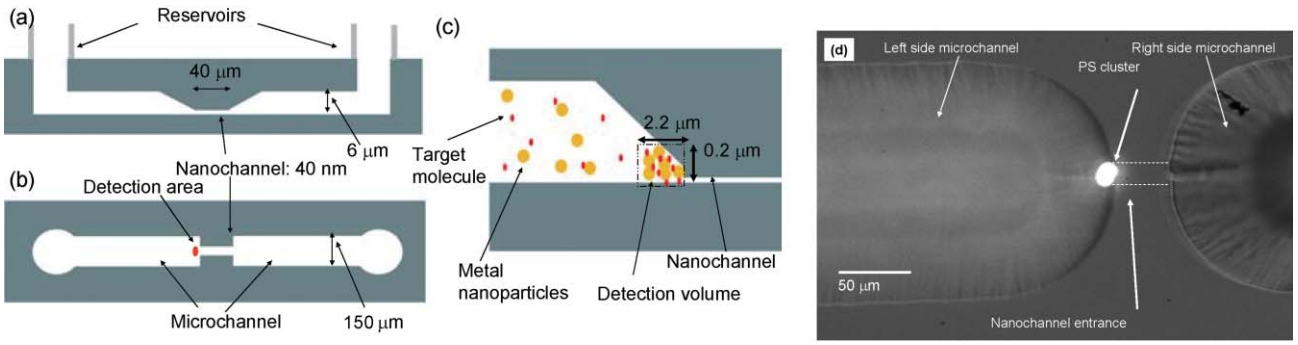

Fig. 1 Schematic diagram of an optofluidic device: (a) side view, (b) top view, (c) side view of an optofluidic device with aggregated nanoparticle-SERS active clusters at the step structure. The depth of nanochannel is smaller than that of nanoparticles. Thus, nanoparticles are trapped and aggregated. (d) Fluorescent image of polystyrene nanoparticles trapped at the step boundary of the optofluidic device.

nanoparticles in aqueous solution (Spherotech Inc., IL) with a size ranging from 40–90 nm were introduced into the optofluidic device. Since the diameter of the fluorescent nanoparticles is larger than the depth of shallow nanochannel, they were trapped at the nanochannel entrance. The solution of PS beads was diluted to 5 mg l^{-1} using deionized (DI) water and then introduced into the nanochannel from the reservoir on the left side. Due to capillary force, the solution was transported into the device within a few seconds. The fluorescent image of PS particles trapped at the entrance of the nanochannel is shown in Fig. 1(d) immediately after the dispensing of the solution. The PS particles emitted extremely high fluorescent signals around the entrance compared to other locations in the microchannel region. The details of investigations about the formation of gold nanoparticle clusters at the entrance of the nanochannel are shown in the ESI.† To investigate channel clogging by the aggregated nanoparticles, 12 μM Rhodamine B in DI water was dispensed into the channel after the PS nanoparticle cluster had been formed at the entrance of the nanochannel. The fluorescent signal from Rhodamine B was observed at both the left and right side of the microchannels This concluded that there were tiny intersticies at the entrance of the nanochannel after the formation of particle clusters and a weak capillary flow could be used to transport Rhodamin B molecules through the cluster and nanochannel site.

To assess this device, the enhancement factor of these nanoparticle clusters were estimated and compared to other SERS techniques using adenine as an analyte. The excitation laser was focused at the nanochannel entrance to obtain the surface enhanced Raman spectra of adenine molecules. SERS detection was accomplished using a Renishaw System 1000 Raman Spectrometer coupled to a Leica DMLM microscope (Schaunberg, IL). The excitation laser source had a wavelength at 785 nm and a power of 8 mW at the sample. A 50× objective lens was used with a spot size of 2.2 μm. The integration time was set to be 2 min and the wave-number range was from 504 cm^{-1} to 1076 cm^{-1}.

There are three signals of adenine molecules shown in Fig. 2. As the reference, graph A shows the Raman signal from a solution of 22 mM adenine on a glass surface without any nanoparticles. It was diluted in a blend of ethanol and DI water. The concentration of ethanol was 10.4 M. Both the

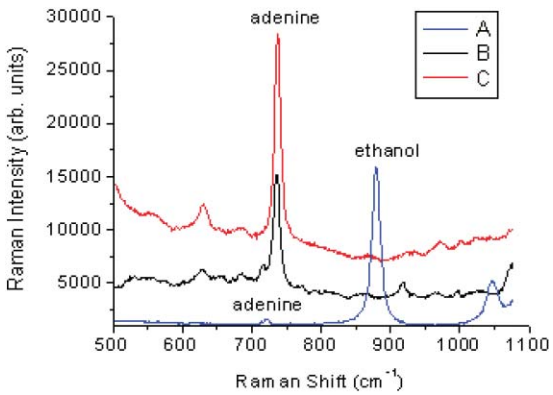

Fig. 2 SERS signals of adenine molecule obtained by (A) SERS active clusters created in an optofluidic device, (B) SERS active clusters made by the conventional chemical method, (C) Raman signal without SERS active clusters.

adenine and ethanol peaks are shown in the Raman spectrum. The intensity of the signal with arbitrary units shows the fingerprint peak at 735 cm^{-1} for adenine. Graph B shows the signal from a solution of 3.33 μM adenine using a conventional colloidal gold SERS technique. The sample was prepared by blending with 0.5 M sodium chloride, which is an activation agent to make the gold nanoparticles aggregate.[5,8–11] After the mixing process, it took 15 min for gold nanoparticles to aggregate into clusters. Graph C shows the Raman signal from 3.33 μM adenine with the use of an optofluidic device. The SERS signal was detected immediately after the sample was dispensed into the channel by capillary force. As depicted, the SERS signal from the optofluidic device is the highest of the three SERS approaches. Using graph A as the reference and the general calculation method,[14] the enhancement factor of the SERS clusters created in the optofluidic device was calculated to be 10^8. From graph B and using same calculation method, the enhancement factor of the conventional method is 10^6.

The SERS signal as a function of time has also been investigated. Due to continuous capillary flow, the concentration of nanoparticles, as well as analytes, at the nanochannel entrance are increased over time. The concept is that, after the nanoparticle–molecule SERS clusters are formed at the entrance of the nanochannel, nanoparticles and moleclues

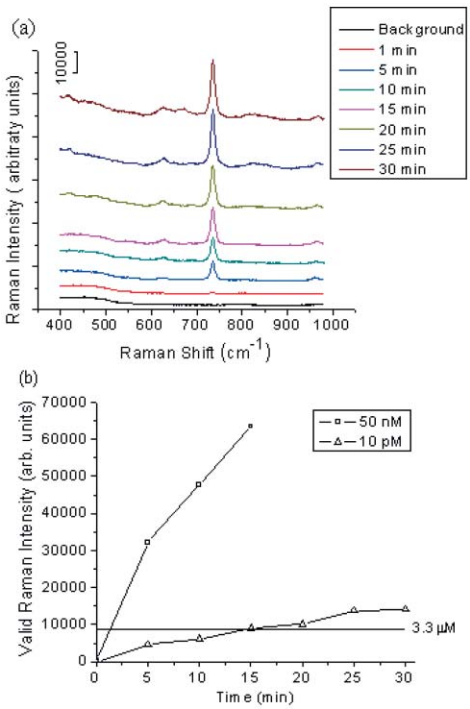

Fig. 3 (a) SERS signal from 10 pM adenine collected at different times after the loading of the sample. (b) SERS signal from 10 pM adenine and 50 nM adenine monitored as a function of time.

continue to flow into the nanochannel entrance and the number of SERS active sites is increased due to continued capillary force. This effect raises the SERS signal intensity. To demonstrate this molecular and nanoparticle enrichment effect, we monitored the SERS signal of adenine over time. The trapping effect of gold colloids and molecules can be stably maintained within 30 min after loading the sample solution into the reservoir. SERS signals of adenine molecules were measurable with a high signal to noise ratio to a concentration as low as 10 pM. The laser with a spot size of 2.2 μm was focused at the entrance of the nanochannel. The integration time of the Raman system was set to 1 min throughout these experiments. The formation of gold clusters with a dimension of more than 10 μm was observed after sample solution dispersion. Fig. 3(a) shows the enhanced Raman signal from a 10 pM adenine solution monitored over 30 minutes after loading the sample solution into the reservoir. Capillary force transported gold nanoparticles and adenine molecules into the nanochannel entrance. Fig. 3(b) shows how the SERS signal intensity of adenine changed over time. Two adenine samples at different concentrations, 50 nM and 10 pM, were investigated. The signal from the 50 nM adenine sample increased and was saturated after 15 minutes. The SERS signal intensity of a 3.3 μM adenine concentration, immediately after loading the adenine solution into the device, is shown as the solid curve in the graph. As depicted, the signal from 10 pM adenine surpassed that of 3.3 μM adenine after 15 minutes. From this, we can reasonably conclude that the enrichment of gold nanoparticles and adenine near the entrance of the nanochannel is increased over time.

After 25 minutes, there is no obvious increase in the concentration because the fluidic flow was terminated. By comparing the final SERS signal intensity of 10 pM adenine to the reference line of 3.3 μM adenine, we can conclude that a more than 10^5 fold increase due to enriched nanoparticle–molecule concentration can be accomplished by this opto-fluidic device. The SERS enhancement reproducibility device to device for adenine with 83 nM is $\pm 10\%$. This is due to the inconsistency of the capillary flow. Now we are investigating the usage of a pumping system to create a constant flow.

In summary, an optofluidic device was fabricated with standard photolithography and etching techniques. Unlike other SERS techniques, this approach offers construction of a metal nanoparticle based SERS active site with a predictable position and with increased local concentration of nanoparticles as well as target molecules. Our optofluidic approach makes the detection much more effective, efficient and rapid. This technique presents the expansion of potential applications including the detection of trace molecules for *in vitro* medical diagnosis, pharmaceuticals testing, or identification of dangerous biological or chemical warfare agents.

References

1 J. R. Ferraro, K. Nakamoto and C. W. Brown, *Introduction of Raman Spectroscopy*, Academic Press, San Diego, CA, USA, 2003.
2 K. Kneipp, H. Kneipp, I. Itzkan, R. R. Dasari and M. S. Feld, *J. Phys.: Condens. Matter*, 2002, **14**, R597.
3 C. Ruan, W. Wang and B. Gu, *Anal. Chem*, 2006, **78**, 3379.
4 S. Nie and S. R. Emory, *Science*, 2002, **275**, 1102.
5 K. Kneipp, Y. Wang, H. Kneipp, L. T. Perelman, I. Itzkan, R. R. Dasari and M. S. Feld, *Phys. Rev. Lett.*, 1997, **78**, 1667.
6 L. Seballos, J. Z. Zhang and R. Sutphen, *Anal. Bioanal. Chem.*, 2005, **383**, 763.
7 Y. C. Cao, R. Jin and C. A. Mirkin, *Science*, 2002, **297**, 1536.
8 N. Félidj, S. L. Truong, J. Aubard, G. Lévi, J. R. Krenn, A. Hohenau, A. Leitner and F. R. Aussenegg, *J. Chem. Phys.*, 2004, **120**, 7141.
9 P. Etchegoin, R. C. Maher, L. F. Cohen, H. Hartigan, R. J. C. Brown, M. J. T. Milton and J. C. Gallop, *Chem. Phys. Lett.*, 2003, **375**, 84.
10 D. L. Jeanmaire and R. P. Van Duyne, *J. Electroanal. Chem. Interfacial Electrochem.*, 1977, **84**, 1.
11 M. Fleischmann, P. J. Hendra and A. J. McQuillan, *Chem. Phys. Lett.*, 1974, **26**, 163.
12 H. Xu, J. Aizpurua, M. Käll and P. Apell, *Phys. Rev. E: Stat. Phys., Plasmas, Fluids, Relat. Interdiscip. Top.*, 2000, **62**, 4318.
13 J. Gersten and A. Nitzan, *J. Chem. Phys.*, 1980, **73**, 3023.
14 Z. Zhu, T. Zhu and Z. Liu, *Nanotechnology*, 2004, **15**, 357.
15 H. Xu, E. J. Bjerneld, M. Käll and L. Börjesson, *Phys. Rev. Lett.*, 1999, **83**, 4357.
16 H. Wang, C. S. Levin and N. J. Halas, *J. Am. Chem. Soc.*, 2005, **127**, 14992.
17 L. Gunnarsson, E. J. Bjerneld, H. Xu, S. Petronis, B. Kasemo and M. Käll, *Appl. Phys. Lett.*, 2001, **78**, 802.
18 N. Félidj, J. Aubard, G. Lévi, J. R. Krenn, A. Hohenau, G. Schider, A. Leitner and F. R. Aussenegg, *Appl. Phys. Lett.*, 2003, **82**, 3095.
19 D. A. Genov, A. K. Sarychev, V. M. Shalaev and A. Wei, *Nano Lett.*, 2004, **4**, 153.
20 Y. Lu, G. L. Liu and L. P. Lee, *Nano Lett.*, 2005, **5**, 5.
21 L. A. Dick, A. D. McFarland, C. L. Haynes and R. P. Van Duyne, *J. Phys. Chem. B*, 2002, **106**, 853.
22 G. L. Liu and L. P. Lee, *Appl. Phys. Lett.*, 2005, **87**, 074101.
23 J. B. Jackson, S. L. Westcott, L. R. Hirsch, J. L. West and N. J. Halas, *App. Phys. Lett.*, 2003, **82**, 257.
24 B. Nikoobakht and M. A. El-Sayed, *J. Phys. Chem. A*, 2003, **107**, 3.